

# LOCALLY GENERATED AND ERROR CHARACTERIZED MTSAT-1R ATMOSPHERIC MOTION VECTORS AND THEIR CONTRIBUTION TO OPERATIONAL NWP IN THE AUSTRALIAN REGION

J. Le Marshall<sup>1,2</sup>, R. Seecamp<sup>3</sup>, M. Dunn<sup>2</sup>, T. Skinner<sup>4</sup>, J. Jung<sup>5</sup>, C. Velden<sup>5</sup>, S. Wanzong<sup>5</sup>, K. Puri<sup>1</sup>, R. Bowen<sup>1</sup>, A. Rea<sup>3</sup>, Yi Xiao<sup>1</sup>, P. Steinle<sup>1</sup>, H. Sims<sup>1</sup> and T. Le<sup>1</sup>

<sup>1</sup> CAWCR, Bureau of Meteorology, Australia, <sup>2</sup> Physics Dept., Latrobe University, Bundoora, Victoria, Australia, <sup>3</sup> OEB, Bureau of Meteorology, Australia, <sup>4</sup> NMOC, Bureau of Meteorology, Australia, <sup>5</sup> CIMSS, University of Wisconsin, Madison, Wisconsin

## Abstract

MTSAT-1R was launched on 26 February 2005 and placed over the Equator at 140° E where it has been operated by the Japanese Meteorological Agency (JMA) as the primary geostationary meteorological satellite, observing the Western Pacific, Asia and the Australian Region. Since 2005, MTSAT-1R data have been received at the Bureau of Meteorology (hereafter referred to as 'the Bureau') satellite groundstation at Crib Point, Victoria, and calibrated and navigated radiance data (imagery) have been used to calculate Atmospheric Motion Vectors (AMVs). The AMVs have been error characterized and used in real time trials to gauge their impact on operational regional Numerical Weather Prediction (NWP). Their benefit is described below. They are used operationally, for analysis in the Darwin Regional Forecast Office and, after these trials, were introduced into the Bureau's National Meteorological and Oceanographic Centre's (NMOC's) operational NWP suite with the upgrade of the Operational Regional Prediction System in October 2007. The MTSAT-1R data are also being tested in the Bureau's next operational NWP system based on the UK Unified Model.

## BACKGROUND

Australia's position in the data sparse southern oceans has resulted in dependence on satellite remote sensing for high quality NWP in our region. AMVs make an important contribution to the satellite data base, for example being one of the most important satellite observations for tropical cyclone track prediction. To provide accurate and timely winds for operational NWP in the Australian Region, AMVs have been calculated locally, from sequential GMS images (Le Marshall et al., 1994, 2002), GOES-9 images (Le Marshall et al., 2004), and now MTSAT-1R images. These have been used to provide AMVs at 15-minute intervals, four times daily, and hourly for the rest of the time. Winds have been generated using infrared (11  $\mu\text{m}$ ), visible (0.5  $\mu\text{m}$ ) and water vapour absorption (6.7  $\mu\text{m}$ ) band images. Here we examine the generation, quality control and application of winds generated from triplets of 15-minute interval infrared imagery every six hours. The hourly generation of winds will allow their use in 4D-Var where their utility for tropical cyclone prediction has already been demonstrated (Le Marshall et al., 1996, 2000a; Leslie et al., 1998).

The methods used at the Bureau, in the past to estimate AMVs, from GMS S-VISSR data, are largely covered in Le Marshall et al. (1999, 2000). Sequential infrared (IR), visible (VIS) or water vapour (WV) band images (a triplet), usually separated by an hour or half an hour were used for velocity estimation. As a result, high density winds were generated continuously at hourly or half hourly intervals. Selected targets in the imagery were tracked automatically using a lagged correlation technique, which minimised root mean square (RMS) differences in brightness from successive pictures to estimate the vector displacement. Cloud height assignment used forecast temperature profiles. The cloud height assigned for low-level clouds was that of the cloud base (following the work of Hasler et al. (1976, 1977)). The benefit of cloud base height assignment is shown in Le Marshall and Pescod (1994). Height assignment involved fitting Hermite polynomials to smooth raw histograms of brightness temperature, enabling estimation of cloud base altitude from cloud base temperature. Upper level AMVs were assigned to the cloud top altitude which was estimated using 11 and 12  $\mu\text{m}$  split window

observations (Le Marshall et al, 1998). For water vapour AMVs, height assignment of the upper and middle-level AMVs in clear conditions was described in Le Marshall et al. (1999). Error characteristics of the AMVs were also determined and each vector was assigned several error indicators, including the Expected Error (EE) and Quality Indicator (QI). The associated correlated error and length scale (Le Marshall et al., 2004a) was also provided.

When GOES-9 replaced GMS-5 in 2003, methods similar to those employed at NESDIS (Daniels et al. 2000) and also at the Bureau (Le Marshall et al. 2000b) were used to generate AMVs from GOES-9 GVAR data received at the Bureau's groundstation at Crib Point (Le Marshall et al., 2004b). In this system, target selection began with a search for tracers using bidirectional brightness temperature gradients in 15 x 15 pixel boxes. Gradients were examined to ensure that cloud edges were being tracked and prospective targets were subjected to a spatial coherence analysis (Coakley and Bretherton, 1982) and tracked using a lagged correlation technique. After tracer selection, three sequential GOES-9 IR images were navigated using matching of land features to ensure that there was consistency between images used for estimating cloud displacement. The height assignment method used for upper level AMVs was based on Schmetz et al. (1993). The technique used was the H<sub>2</sub>O-intercept method, using 11 μm (channel 4) observations and the 6.7μm (channel 3) observations. Radiances from the infrared and water vapour channels were measured and compared to calculate Planck blackbody radiances as a function of cloud top pressure. Cloud top height was then inferred from linear extrapolation of radiances onto the calculated curve of opaque cloud radiances, providing the target altitude. The approach was described in Nieman et al. (1993). The low-level AMV altitude assignment technique was similar to that developed in the Bureau of Meteorology (Le Marshall et al. 2000b) where cloud altitude was assigned to the cloud base for low-level vectors. As with the GMS-5 the error characteristics of the AMVs were determined and each vector was associated with error indicators such as the EE and QI as well as with a correlated error and length scale.

## MTSAT-1R ATMOSPHERIC MOTION VECTORS

When MTSAT-1R replaced GOES-9 in 2005, again, methods similar to those employed at NESDIS (Daniels et al. 2000) and also at the Bureau (Le Marshall et al. 2000b) were used to generate AMVs from the MTSAT-1R HIRID data received at the Crib Point groundstation. Three sequential images from MTSAT-1R were navigated using land features to ensure that there was consistency between images used for estimating cloud displacement. In this system, target selection for infrared (11 μm) targets, commenced with a search for tracers, using bidirectional brightness temperature gradients in 15 x 15 pixel boxes. As with GOES-9, targets with gradient features were subjected to a spatial coherence analysis (Coakley & Bretherton, 1982) and tracked using lagged correlation. Height assignment methods were similar to those employed for GOES-9. The schedule for generating these MTSAT-1R based winds is in Table 1. Figure 1 is an example of the MTSAT-1R IR AMVs generated for 12 UTC on 18 March 2007.

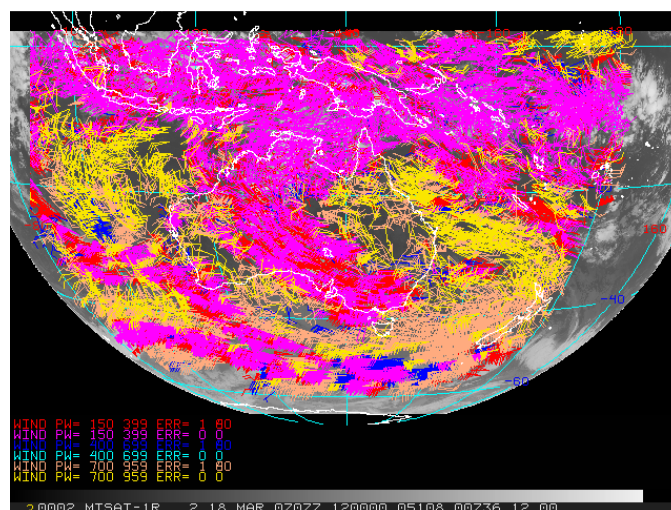


**Fig. 1 MTSAT-1R AMVs generated around 12 UTC on 18 March 2007. Magenta denotes upper level tropospheric vectors, yellow, lower level tropospheric vectors**

**Table 1. Real time schedule for MTSAT-1R Atmospheric Motion Vectors at the Bureau of Meteorology. Sub-satellite image resolution, frequency and time of wind extraction and separations of the image triplets used for wind generation ( $\Delta T$ ) are indicated.**

Wind Type	Resolution	Frequency-Times (UTC)	Image Separation
Real Time IR	4 km	6-hourly – 00, 06, 12, 18	15 minutes
Real Time IR (hourly)	4 km	Hourly – 00, 01, 02, 03, 04, 05, . . . , 23	1 hour

## ACCURACY AND QUALITY CONTROL

Careful quality control (QC) and error characterization ensure the AMVs have a beneficial impact on NWP (Le Marshall et al. 2004a). Error characterization used the Bureau’s initial error flag (ERR), which involved a number of basic checks ( first guess departure check, vector pair acceleration check, tracer constancy check etc. ), the Quality Indicator (QI), (Holmlund et al. 1998) and the more recent Expected Error (EE), (Le Marshall et al. 2004a).

These error indicators are used to effectively thin the AMVs and to ensure good data coverage with average separations exceeding the Length Scale of the Correlated Error. The thinning methodology has also ensured that the errors are not significantly larger than the background error field of the forecast model measured at radiosonde sites. The approach is detailed in Le Marshall et al. (1994a).

The Expected Error (EE) has several components, the total RMS error (m/s) currently used operationally, the meridional and the zonal error components (m/s), the vector height error (hPa) and the error in the wind vector determination (m/s), often due to navigation and tracking related inaccuracies. The Expected Error generated for MTSAT-1R has been used in these studies. The first component of the EE, the total RMS error (which is currently determined statistically for operational application) has recently been placed in the BUFR code used by test forecast systems (eg. at NOAA/NESDIS as the quality indicator *EE*, derived from EE(1) the Total RMS error, where

$$\text{BUFR } EE = (100 - 10.0 * EE(1)) \quad (1)$$

A typical comparison of the EE (total RMSE) with the actual error for MTSAT-1R IR winds is seen in Figures 2. Here, the EE(total RMSE) has been compared to the actual error determined using contemporaneous radiosonde data within 150 km of the AMVs and is seen to be an effective tool for selecting high quality AMVs.

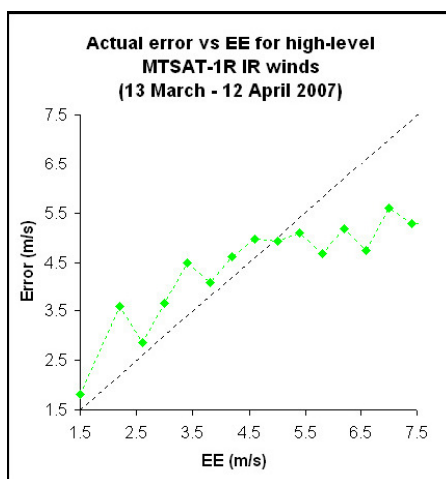


**Fig. 2 (a) Measured error (m/s) versus EE for high-level MTSAT-1R IR winds (13 March - 12 April 2007)**

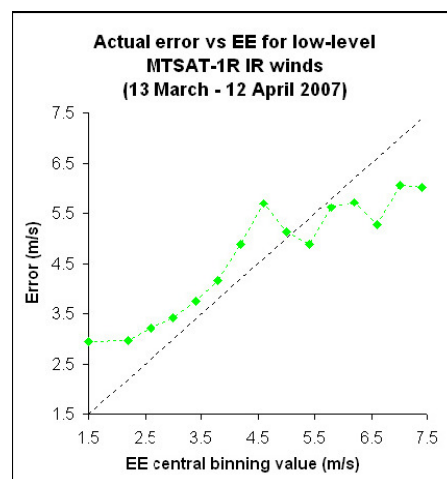


**Fig. 2 (b) Measured error (m/s) versus EE for low-level MTSAT-1R IR winds (13 March - 12 April 2007)**

Quality control of AMVs to provide low, middle and high level data in the BoM system has used all 3 error indicators (EE, QI, ERR). Typical accuracy of the AMVs available for NWP is given in Table 2 which shows the Mean Magnitude of Vector Difference (MMVD) between MTSAT-1R AMVs and radiosondes winds within 150 km in the Australian Region for March 2007.

**Table 2. Mean Magnitude of Vector Difference (MMVD) between MTSAT-1R AMVs, forecast model first guess and radiosonde winds within 150 km for March 2007**

Level	No. of Obs	First Guess MMVD (ms <sup>-1</sup> )	AMV MMVD (ms <sup>-1</sup> )
Low 950 – 700 hPa	192	2.67	2.92
Middle 699 – 400 hPa	88	3.79	3.75
High 399 – 150 hPa	706	4.13	4.08

## CORRELATED ERROR

As with earlier geostationary satellite local AMV systems, the correlated error has been analysed for the Bureau produced MTSAT-1R winds (Le Marshall et al., 2004a). The correlated error and its spatial variation (length scale) were determined using the Second Order Auto Regressive (SOAR) function :

$$R(r) = R_{00} + R_0(1 + r/L) \exp(-r/L) \quad (2)$$

where  $R(r)$  is the error correlation,  $R_0$  and  $R_{00}$  are the fitting parameters (greater than 0),  $L$  is the length scale and  $r$  is the separation of the correlates. Thus, the difference between AMV and radiosonde winds (error) has been separated into correlated and non-correlated parts. A typical variation of error correlation with distance for MTSAT-1R IR1 AMVs is seen in Fig. 3, while the parameters of the SOAR function which best fits the observations are in Table 3.

These length scales may be compared to those from GMS-5, namely, 123 km and 73 km, for low and high levels respectively, where the GMS-5 vectors were subjected to a quality control regime close to that of  $EE < 6$ .

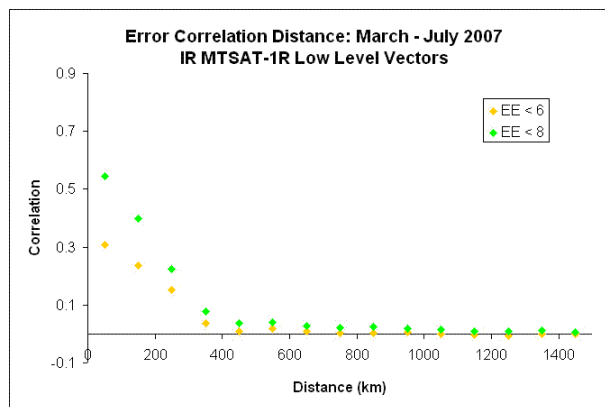


**Fig. 3 Error correlation versus distance (100 km bins) for low-level MTSAT-1R AMVs with  $EE < 6$  and  $8 \text{ m/s}$  (March – July 2007)**

**Table 3. Parameters of the SOAR function (Equation 2) which best model the measured error correlations for the MTSAT-1R AMVs listed in the left column of the table. (February – April, 2007)**

MTSAT-1R IR1 AMVS	$R_{00}$		$R_0$		$L$ (km)	
	Low	High	Low	High	Low	High
$EE$ (RMSE) < 6	0.006	0.370	0.460	0.460	86.000	99.900
$EE$ (RMSE) < 8	0.066	0.052	0.640	0.440	122.700	110.900

## REAL TIME ASSIMILATION TRIALS

Before local MTSAT-1R data could be incorporated into the Bureau's operational NWP suite, real time assimilation trials using MTSAT-1R infrared channel 1 (IR1) AMVs were undertaken using the then current operational LAPS system of March 2007 configured to run at  $0.375^\circ$  horizontal resolution with 51 levels in the vertical. The system and methodology are described below. A trial was also conducted

using the Bureau's next (October 2007) operational LAPS system with 61 vertical levels and 0.375° resolution. *The results from both tests were similar and consistent with earlier results from assimilation of GMS-5 and GOES-9 local vectors* (e.g. Le Marshall et al., 2002; Le Marshall et al., 2004b).

## THE ASSIMILATION SYSTEM

The assimilation methodology employed the real time operational NMOC regional Limited Area Prediction System, using all available data (including all available JMA AMVs) as the control. The analyses on which the forecasts reported here are based start with a Bureau Global Analysis and Prognosis System (GASP) global analysis (Seaman et al. 1995), valid 12 hours prior to the forecast start time. This is used as a first guess to the regional analysis which then provides the base analysis for an initialised six hour forecast, a subsequent analysis and a further initialised six hour forecast. This forecast is then used as a first guess to the final analysis from which the 24 and 48 hour forecasts are run. Forecasts are nested in fields from the most recent GASP forecast (Bourke et al. 1995).

## THE ANALYSIS AND FORECAST MODELS

The LAPS analysis and forecast model uses a common latitude/longitude/sigma coordinate system. The configuration consisted of 320 x 220 gridpoints at 0.375° spacing in the horizontal, and 51 levels (L51) in the vertical, with an upper level of sigma 0.01. A second version of the LAPS with 61 levels (L61) in the vertical and an upper sigma level of 0.0001 was also used in these tests. The analysis system was a limited area adaptation of the global multivariate statistical interpolation analysis (Seaman et al. 1995). The errors assigned to the atmospheric motion vectors in the operational analysis scheme are 3 ms<sup>-1</sup>, 4 ms<sup>-1</sup> and 5 ms<sup>-1</sup> for low, middle and high level vectors respectively. These numbers are consistent with the errors of 3 ms<sup>-1</sup> assigned to local middle and high level radiosonde observations and the differences between collocated local AMVs and radiosonde wind estimates usually recorded at the Bureau.

The forecast model is described in Puri et al. (1998) and is a hydrostatic model formulated in latitude/longitude/sigma coordinates on the Arakawa A-grid. It uses high order numerics and includes a comprehensive physics package and the digital filter initialisation of Lynch and Huang (1992).

## METHOD

In the real time trial MTSAT-1R AMVs generated using 11 µm (Channel IR1) and 6.7 µm (Channel IR3) imagery was added to the operational regional assimilation system. The operational regional NWP system already contains AMVs from the Japanese Meteorological Agency, available up to the operational cut-off time (analysis time + 1.75 hours; 0.75 hours when daylight saving applies), which may preclude on time vectors. The methodology was similar to that used in Le Marshall et al. (2002). The accuracy of the real time AMVs provided to the assimilation system for the period studied in the first experiment with L51 LAPS in mid-2007 is summarised in Table 4. It shows the mean magnitude of vector difference and RMS difference between AMVs and radiosondes within 150 km, and, in

**Table 4. Mean Magnitude of Vector Difference (MMVD) and Root Mean Square Difference (RMSD) between MTSAT-1R AMVs, forecast model first guess winds and radiosonde winds for the period 30 May to 15 June 2007**

Level	Data Source	Bias (ms <sup>-1</sup> )	No. of Obs	MMVD (ms <sup>-1</sup> )	RMSVD (ms <sup>-1</sup> )
High – up to 150 km separation between radiosondes and AMVs	AMVs	-0.55	1386	3.90	4.47
	First Guess	1.3776	1386	4.42	5.09
Low - up to 150 km separation between radiosondes and AMVs	AMVs	-0.76	540	3.18	3.72
	First Guess	-0.70	540	2.72	3.12
Low – up to 30 km separation between radiosondes and AMVs	AMVs	-0.44	18	2.45	3.08
	First Guess	-0.20	18	2.67	3.07

the case of low-level vectors between AMVs and radiosonde at 150 km and also at 30 km separation. It can be seen that, the accuracy of the local AMVs at radiosonde sites is better than that of the forecast model first guess field used when calculating the winds, although, for low level vectors, a more stringent collocation criterion between the AMVs and the radiosondes for calculating errors was required for this to be the case. In this study, local quality control methods were used to provide vectors with expected error consistent with the error levels anticipated for AMVs in the operational analysis. The data used for this operational trial was generated from triplets of IR and WV images centred at 00, 06, 12 and 18 UTC where the images used were separated by 15 minutes. The system provided AMV coverage and accuracy consistent with the correlated error length scale and expected error, and the resolution characteristics of the data and data assimilation system.

A series of parallel *real time* forecasts was run using the operational forecast system with AMV data added to the operational database, which included all available MTSAT-1R AMVs from JMA. The experimental period was from 00 UTC 30 May to 12 UTC 15 June 2007 (34 cases). The experimental period was relatively short but encompassed a variety of synoptic patterns in the Australian Region, including blocking sequences in the Tasman Sea. For these real time forecasts, the S1 skill scores (Teweles, and Wobus, 1954) were calculated on the NMOC operational verification grid using 00 UTC and 12 UTC analyses. The verification grid consists of 58 points within the domain 90° E to 170° E, 15° S to 55° S. The exact grid is seen in Bennett and Leslie (1981).

A test was also conducted 1 September to 8 October 2007 (72 cases), using the next (now current) operational version of LAPS. The significant changes to the LAPS system with this implementation are an extension to 61 levels (L61) in the vertical and the reinstatement of local direct readout ATOVS.

## RESULTS

The S1 skill scores for 24-hour forecasts from using MTSAT-1R AMV data in the May 2007 operational (L51) LAPS model are compared to the operational skill scores in Table 5 (a). The statistics are consistent with those recorded in earlier impact studies with GMS-5 (Le Marshall et al. 2002) and GOES-9 (Le Marshall et al., 2004) where a modest positive impact, mainly in the lower levels, was recorded. The S1 skill scores for the new L61 LAPS (72 cases) are in Table 5(b). A positive impact consistent with previous results for local GMS-5 and GOES-9 AMVs was again recorded.

These results show that real time MTSAT-1R IR and WV image based AMVs, are of an accuracy which can benefit operational NWP in the Australian Region. Addition of the vectors to the operational regional forecast system which already contains some JMA AMVs, has provided both improved data coverage of the region and small average forecast improvement. The results and their consistency with previous studies has led to a reintroduction of these local AMVs into operational use.

Table 5 (a) 24 hr forecast verification S1 Skill Scores for the May 2007 operational regional forecast system (L51 LAPS) and L51 LAPS with IR, 6-hourly image based AMVs for 30 May to 15 June 2007 (34 cases)			Table 5 (b) 24 hr forecast verification S1 Skill Scores for the next operational regional forecast system (L61 LAPS) and L61 LAPS with IR, 6-hourly image based AMVs for 1 September to 8 October 2007 (72 cases)		
LEVEL	(LAPS) S1	(LAPS + MTSAT-1R AMVS) S1	LEVEL	(LAPS) S1	(LAPS + MTSAT-1R AMVS) S1
MSLP	19.00	18.81	MSLP	20.24	19.15
1000 hPa	21.35	20.80	1000 hPa	20.06	19.13
900 hPa	22.42	22.08	900 hPa	18.65	17.75
850 hPa	22.81	22.76	850 hPa	17.41	16.69
500 hPa	15.96	15.91	500 hPa	12.41	11.73
300 hPa	13.65	13.65	300 hPa	10.49	9.76
250 hPa	12.62	12.58	250 hPa	12.41	11.90

## THE FUTURE

The Bureau of Meteorology is now transitioning to the use of the United Kingdom Unified Model (UKUM) for operational forecasting over the global and regional domain. As part of this process, forecasts are being performed in the Australian Region using the full real-time database now available within the region, which includes local continuous (hourly) error characterized AMVs. Recently these high-density hourly visible and infrared image-based winds (see Figure 4) have been used in a series of experiments examining the motion of tropical cyclone Nicholas which developed off the NW coast of Australia during February 2008. The forecasts shown here were undertaken using the UKUM at 37.5km resolution employing four dimensional variational assimilation (4D-VAR) with a six-hour time window. A sample forecast is seen in Figure 4 (b), (c) and (d). The 12, 24 and 36-hour forecasts for tropical cyclone Nicholas from 12UTC on the 14 February 2008 are shown and represent high standard operational guidance for track and intensity in what was a difficult forecast case. Further work continues with these and other regional and global studies and results indicate the potential for significant improvement in operational guidance on implementation of the system.

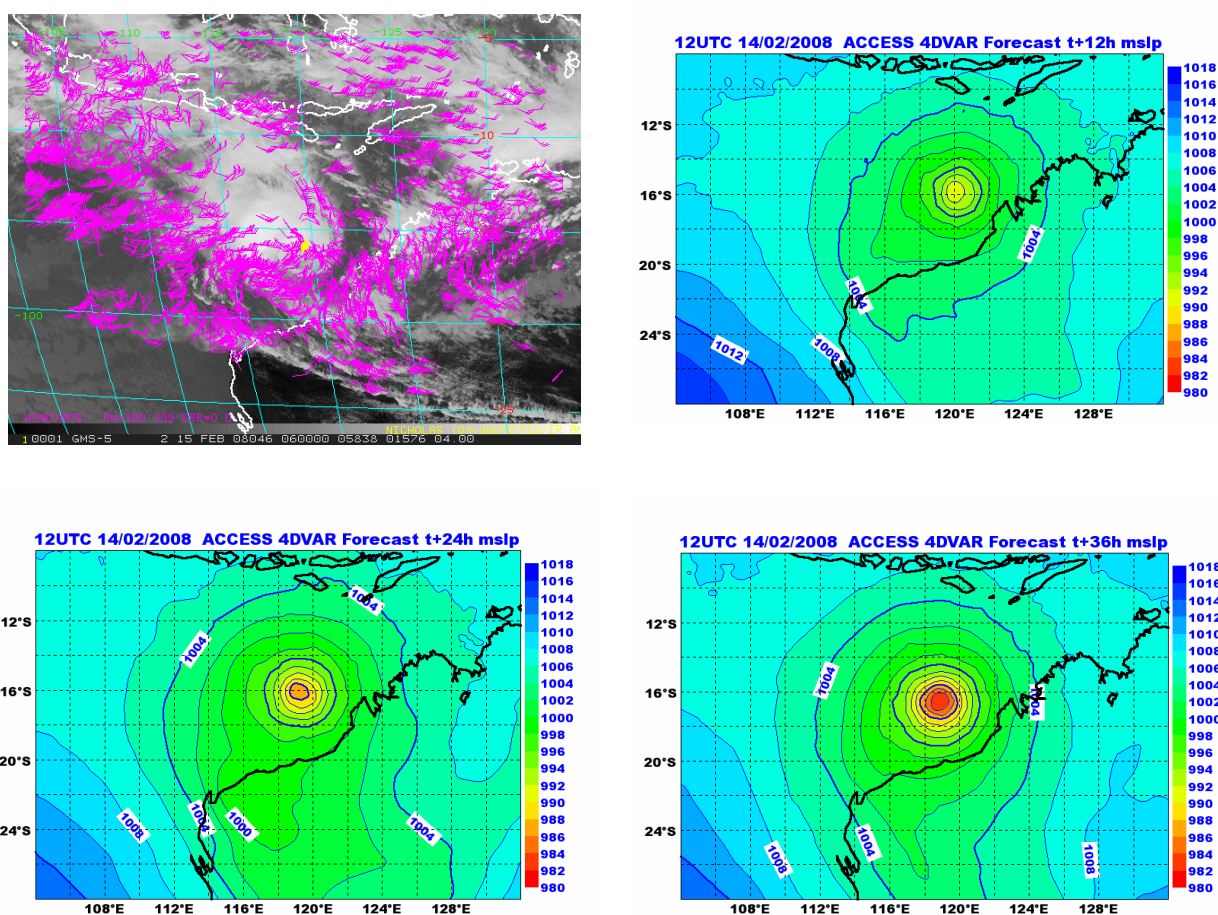


Figure 4. (a)Upper tropospheric visible and infrared image-based hourly AMVs for the period 4 - 8 UTC on 15 February 2008 near TC Nicholas (yellow dot) and the 12 (b), 24 (c) and 36-hour (d) 4D-VAR forecasts from the UKUM starting 12 UTC on 14 February 2008.

## SUMMARY AND CONCLUSIONS

The local estimation of real time operational MTSAT-1R AMVs and their impact on operational regional NWP has been described. Experiments using these data in a real time NWP trial have been summarized. Their benefit to current operational regional NWP, when used with a control employing NMOC's full operational data base (including JMA AMVs), has been recorded. These results were

consistent with past trials with GMS-5 and GOES-9 and have resulted in a reintroduction of local AMVs into operations.

This trial has been followed by new studies of the impact of 6-hourly Visible image-based AMVs and hourly IR and Visible AMVs, in the current operational systems and a study of the use of continuous (at least hourly) AMVs in the next generation 4-D VAR United Kingdom Meteorological Office Unified Model based system. Initial results from these experiments are promising.

Looking ahead, the continuing trend to space-based observations with higher spatial, temporal and spectral resolution should enable improved estimation of atmospheric motion and result in quantitative benefit to NWP. In the near future, the prospects of benefits from the expanded use of sequential observations from MTSAT-1R, MTSAT-2 and the Chinese satellite, FY-2 and also from next generation ultraspectral instruments such as the Geostationary Imaging Fourier Transform Spectrometer (Smith et al. 2000) are very good.

## Acknowledgements

Thanks are due to Bert Berzins, Ian Senior and Weiqing Qu for assistance in data access and to Terry Adair for assistance in the preparation of this manuscript.

## REFERENCES

- Bennett, A.F. and Leslie, L.M. 1981. Statistical Correction of the Australian Region Primitive Equation Model *Mon. Wea. Rev.* **109**, 453 – 462.
- Bourke, W.P., Hart, T., Steinle, P., Seaman, R., Embery, G., Naughton, M. and Rikus, L. 1995. Evolution of the Bureau of Meteorology's Global Assimilation and Prediction System. Part 2 : Resolution enhancements and case studies. *Aust. Met. Mag.* **44**, 19 - 40.
- Coakley, J. and F. Bretherton. 1982. Cloud cover from high resolution scanner data : Detecting and allowing for partially filled fields of view. *J. Geophys. Res.* **87**(C7), 4917 – 4932.
- Daniels, J., Velden, C., Busby, W. and Irving, A. 2000. Status and Development of Operational GOES Wind Products. *Proc. Fifth International Winds Workshop, Lorne, Australia, 28 – 31 March 2000*. Published by EUMETSAT EUM P28 ISSN 1023-0414. 27 – 45.
- Hasler, A. F. Shenk, W. and Skillman, W. 1976. Wind estimates from cloud motions: Phase 1 of an in situ aircraft verification experiment *J. Appl. Meteor.* **15**, 10 – 15.
- Hasler, A.F., Shenk, W. and Skillman, W. 1977. Wind estimates for cloud motions: preliminary results of phase I, II and III of an in situ aircraft verification experiment, *J. Appl. Meteor.* **16**, 812 - 815.
- Holmlund, K., 1998. The utilization of statistical properties of satellite-derived atmospheric motion vectors to derive quality indicators, *Wea. Forecast.*, **13**, 1093 – 1104.
- Le Marshall, J.F., Pescod, N., Seaman, R., Mills, G. and Stewart, P. 1994. An Operational System for Generating Cloud Drift Winds in the Australian Region and Their Impact on Numerical Weather Prediction. *Weath. Forecasting*, **9**, 361 - 370.
- Le Marshall, J.F. and Pescod, N. 1994. Generation and application of cloud drift winds in the Australian Region - recent advances. *Proceedings of the Pacific Ocean Remote Sensing Conference, Melbourne, Australia, 1 - 4 March, 1994*, 467 - 474.
- Le Marshall, J.F., Leslie, L.M. and Bennett, A.F. 1996. Tropical cyclone Beti - an example of the benefits of assimilating hourly satellite wind data. *Aust. Met. Mag.* **45**(4), 275 - 284
- Le Marshall, J.F., Pescod, N., Seecamp, R., Spinoso, C. and Rea, A. 1998. Improved Weather Forecasts from Continuous Generation and Assimilation of High Spatial and Temporal Resolution Winds. *Proc. Fourth International Winds Workshop, Saanenmoser, Switzerland, 20 - 24 October, 1998*. 101 - 108.
- Le Marshall, J.F., Pescod, N., Seecamp, R., Puri, K., Spinoso, C. and Bowen, R. 1999. Local estimation of GMS-5 water vapour motion vectors and their application to Australian region numerical weather prediction. *Aust. Met. Mag.* **48**, 73 - 77.
- Le Marshall, J., Leslie, L., Morison, R., Pescod, N., Seecamp, R. and Spinoso, C. 2000a. Recent Developments in the Continuous Assimilation of Satellite Wind Data for Tropical Cyclone Track Forecasting. *Adv. Space Res.* **25**(5), 1077 - 1080.
- Le Marshall, J.F., Pescod, N., Seecamp, R., Rea, A., Tingwell, C., Ellis, G. and Shi, H. 2000b. Recent Advances in the quantitative generation and assimilation of high spatial and temporal



- resolution satellite winds. *Proc. Fifth International Winds Workshop, Lorne, Australia, 28 – 31 March 2000*. Published by EUMETSAT EUM P28 ISSN 1023-0414. 47 – 56.
- Le Marshall, J., Mills, G., Pescod, N., Seecamp, R., Puri, K., Stewart, P., Leslie, L.M. and Rea, A. 2002. The estimation of high density atmospheric motion vectors and their application to operational numerical weather prediction. *Aust. Met. Mag.* **51**, 173 – 180.
- Le Marshall, J., Rea, A., Leslie, L., Seecamp, R. and Dunn, M. 2004a. Error Characterization of Atmospheric Motion Vectors. *Aust. Met. Mag.* **53(2)**, 123 – 131.
- Le Marshall, J., Seecamp, R., Daniels, J., Velden, C., Puri, K., Bowen, R., Rea, A. and Dunn, M. 2004b. The contribution of GOES 9 to operational NWP forecast skill in the Australian region. *Aust. Met. Mag.* **53(4)**, 279 – 283.
- Leslie, L. M., Le Marshall, J. F., Morison, R. P., Spinoso, C., Purser, R. J. Pescod, N. and Seecamp, R. 1998. Improved Hurricane Track Forecasting from the Continuous Assimilation of High Quality Satellite Wind Data. *Mon. Wea. Rev.* **126(5)**, 1248 – 1258.
- Lynch, P and Huang, X-Y. 1992. Initialization of the HIRLAM Model using a digital filter. *Mon. Wea. Rev.* **120**, 1019 – 1034.
- Nieman, S., Schmetz, J. and Menzel, W.P. 1993. A comparison of several techniques to assign heights to cloud tracers. *J. Appl. Meteor.* **32**, 1559 – 1568.
- Puri, K., Dietachmeyer, G., Mills, G.A., Davidson, N.E., Bowen, R.M. and Logan L.W. 1998. The new BMRC Limited Area Prediction System, LAPS. *Aust. Met. Mag.* **47**, 203 - 223.
- Schmetz, J., Holmlund, K., Hoffman, J., Strauss, B., Mason, B., Gaertner, V., Koch, A. and Van De Berg, L. 1993. Operational cloud motion winds from METEOSAT infrared images. *J. Appl. Meteor.* **32**, 1206 – 1255.
- Seaman, R., Bourke, W., Steinle, P., Hart, T., Embery, G., Naughton, M. and Rikus, L. 1995. Evolution of the Bureau of Meteorology's Global Assimilation and Prediction system. Part 1: analysis and initialisation. *Aust. Met. Mag.* **44**, 1 - 18.
- Smith, W.L., Harrison, F.W., Revercomb, H.E., Bingham, G.E., Huang H.L. and Le Marshall, J.F. 2000. The Geostationary Imaging Fourier Transform Spectrometer. *Proc. Eleventh International TOVS Study Conference, Budapest, Hungary*. 391 - 398.
- Teweles, S. and Wobus, H. 1954. Verification of Prognostic Charts. *Bull. Amer. Meteor. Soc.* **35**, 455 - 463.